

# Application of GIS and Google Earth Engine to Assess Built-up Area Changes during Urbanization in Hai Duong City, Hai Duong Province, Vietnam

Long, N. B.,<sup>1</sup> Oanh, N. T.<sup>2\*</sup> and Dinh, N. T.<sup>3</sup>

College of Land Management and Rural Development, Viet Nam National University of Forestry, Vietnam

E-mail: longnb@vnuf.edu.vn,<sup>1</sup> oanhnt@vnuf.edu.vn,<sup>2</sup> dinhnt@vnuf.edu.vn<sup>3</sup>

\*Corresponding Author

DOI: <https://doi.org/10.52939/ijg.v21i11.4599>

## Abstract

Monitoring changes in built-up areas is essential for understanding urban growth, reducing environmental impacts, and guiding sustainable land-use planning. This study investigates the changes in built-up areas in Hai Duong City from 2000 to 2020. Landsat 5 and Landsat 8 imagery were utilized on the Google Earth Engine platform, integrated with GIS analysis to assess these changes. The study employed several indices, including the Normalized Difference Built-up Index (NDBI), Soil Adjusted Vegetation Index (SAVI), and Modified Normalized Difference Water Index (MNDWI), to calculate the Built-up Index (BI), which serves as an efficient tool for classifying built-up areas. The results indicated that the built-up areas in 2000, 2010, and 2020 were 474.04 ha, 1,497.32 ha, and 4,432.83 ha, respectively, with overall accuracy ranging from 89% to 92% and Kappa coefficients between 0.76 and 0.80. Ngoc Chau, Thanh Binh, and Tan Binh Wards recorded built-up land expansion between 2000 and 2020 exceeding 70% of their total natural area, with respective increases of 143.15 ha, 192.43 ha, and 199.47 ha. The findings of this study provide a robust scientific foundation for urban planning in Hai Duong City, Hai Duong Province, and support policymakers in formulating sustainable development strategies aimed at improving the quality of urban life.

**Keywords:** Built-up Expansion, Built-up Index, Landsat, Remote Sensing, Google Cloud Platform

## 1. Introduction

The urbanization process of a country includes two processes, which are the expansion of existing urban areas and the formation of new urban areas [1]. This has changed the characteristics of the urban ecosystem, which is reflected in the transformation of the space of the land cover from natural ecosystems to ecosystems affected by humans [2]. The urbanization changes land use in urbanized areas and adjacent areas. The area of agricultural land and unused land decreases, while the area of non-agricultural land increases [3] and [4]. In addition, infrastructure construction is inseparable from the urbanization process, leading to a rapid increase in the area of built-up areas. Therefore, monitoring and supervising changes in built-up area plays an important role in monitoring the urbanization process.

The analysis and detection of changes in land use using remote sensing (RS) and GIS technology have been successfully applied in many countries around the world. In the 1970s and 1980s, studies began to use remote sensing data to collect data on land-use

and land-cover [5], land use planning [6], and land use changes [7]. These research groups have proposed methods and techniques for using remote sensing data to monitor and evaluate land use changes. Traditional methods for land cover mapping, such as field surveys, aerial photo interpretation, and manual digitization, have long provided reliable and detailed information at local scales [8]. Despite their usefulness, these approaches are time-consuming, labor-intensive, and difficult to update consistently across large areas or long time periods [9]. In tropical regions, persistent cloud cover and complex landscapes further reduce the effectiveness of conventional mapping techniques [10]. Moreover, the growing demand for timely and consistent land cover information has highlighted the limitations of traditional practices compared with modern satellite-based approaches [11] and [12]. To address these challenges, recent studies have increasingly adopted cloud-based platforms and open-access satellite archives.

Google Earth Engine (GEE) has emerged as a powerful platform for large-scale and long-term monitoring of land cover dynamics, offering efficient, consistent, and reproducible analysis [11]. By integrating multi-temporal satellite imagery with advanced geospatial techniques, GEE reduces time and labor while providing timely insights essential for urban planning, environmental management, and sustainable development [13] and [14]. Recent studies confirm that combining GEE with GIS enables rapid processing of large-scale datasets and advanced data mining, revolutionizing traditional RS data processing and analysis frameworks [15] and [16]. The application of GEE and RS imagery were used in urban expansion model, buffer zone analysis, quadrant division in GIS, and principal component analysis to examine urban growth in Chengdu, China, and revealed accelerated but spatially and temporally heterogeneous expansion patterns [17]. Alongside these advances, spectral indices have been widely applied worldwide to identify built-up areas in multispectral imagery, demonstrating both effectiveness and accuracy. Numerous studies have highlighted the advantages of indices such as the NDBI, IBI, Normalized Difference Vegetation Index (NDVI), and MNDWI for classifying built-up and impervious surfaces during urbanization. By enhancing the distinction between built-up land, vegetation, and water bodies, these indices provide higher classification accuracy and lower cost compared to traditional methods [18][19][20] and [21]. In Vietnam, researchers have successfully applied these methods using Landsat and Sentinel imagery to map urban expansion in cities such as Hanoi, Thanh Hoa, and Bien Hoa, achieving overall accuracies above 87% [22][23] and [24].

A key strength of these indices is their ability to efficiently handle multi-temporal satellite data, enabling long-term monitoring of spatial-temporal urban dynamics. When integrated into cloud-based platforms like GEE, they further enhance scalability, consistency, and reproducibility in built-up land monitoring [13] and [16]. Building on these approaches, this study applies the IBI to extract built-up areas in 2000, 2010, and 2020, using the GEE platform for computation and GIS techniques to analyze spatial and temporal changes in Hai Duong City, Hai Duong Province. The findings are expected to provide valuable information for urban planning and sustainable land management, supporting local authorities in making informed decisions.

## 2. Materials and Methods

### 2.1 Study Area

Hai Duong City is a provincial city located in the center of Hai Duong Province. This is the economic, technical, educational, scientific, medical and service center of Hai Duong Province, 57 km from Hanoi Capital and located in the economic triangle of Hanoi - Hai Phong - Quang Ninh. It has geographical coordinates from 20°43' to 21°14' North latitude, 106°03' to 106°38' East longitude (Figure 1). The city's administrative boundaries include 19 wards and 06 communes with a total area of about 11,168.18 ha [25]. The city is a traffic and exchange hub within the province and inter-provincial regions, and is also one of the industrial centers of the Northern Key Economic Zone, Vietnam. The strong and rapid development of urban space and infrastructure has created a great driving force, promoting the economic development of the city. Hai Duong contributes a large proportion to the province's overall GDP with economic growth for many consecutive years reaching an average of more than 14%/year, ranking among the localities with the highest growth rate in the region.

### 2.2 Data Collection

On the GEE platform, Landsat images were filtered for each target year (2000, 2010, and 2020) using a consistent time window from January 1st to December 31st and were spatially clipped to the administrative boundary of Hai Duong City (Figure 2). Cloud and cloud-shadow pixels were masked using GEE's built-in cloud masking functions, which isolate valid surface observations. The filtered images were then composited using the median reducer to generate a representative image for each year. For 2000, 30 images from Landsat 5 were selected; for 2020, 54 images from Landsat 8 were used. In 2010, although more than 40 Landsat 5 images were available, most exhibited cloud cover exceeding 30%, which would have introduced significant contamination into the composite. Therefore, an additional cloud cover filter (<30%) was applied, resulting in the selection of 12 high-quality images for that year. All selected scenes fall within Path 126 and 127 and Row 45 and 46, ensuring consistent spatial coverage across the study area. The land use status quo map was obtained from the Department of Natural Resources and Environment of Hai Duong City, Hai Duong Province. QGIS software was utilized to analyze changes in built-up areas during the study periods. The study was conducted using the EPSG:9209 – VN-2000 / TM-3 105-30 projected coordinate reference system.

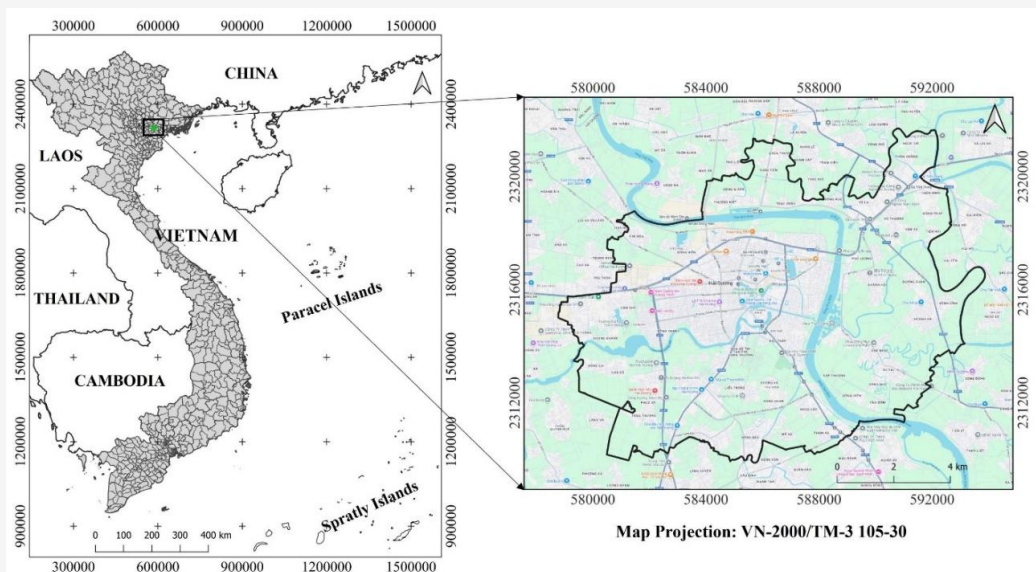


**Figure 1:** Hai Duong City, Hai Duong province, Vietnam

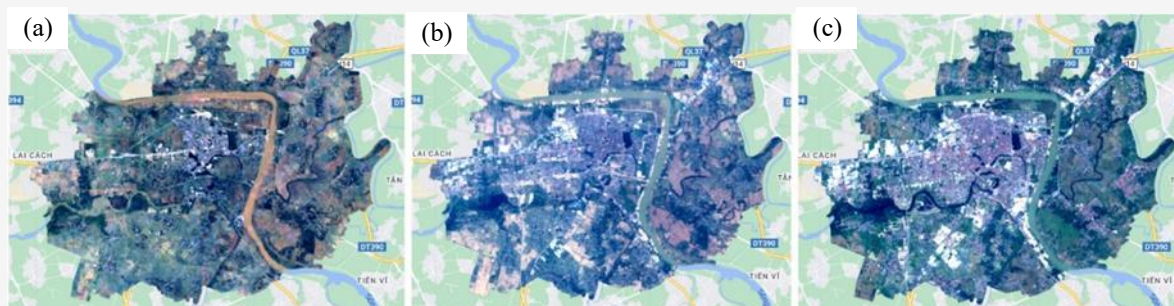


**Figure 2:** Collection of acquired satellite images (a) 2000, (b) 2010, and (c) 2020

### 2.3 Methods

On the GEE platform, a Landsat image collection at three study time points was generated by filtering by date and boundary. Cloud masking was performed using the QA band to remove cloudy and dark areas, and the Median function was applied to synthesize the images, ensuring consistency and reducing noise.

#### 2.3.1 Determine the built-up areas

IBI is an effective tool for the rapid classification of built-up areas, derived from the integration of three spectral indices: NDBI, SAVI, and MNDWI. As a composite indicator, IBI is widely regarded as a clear and direct representation of urbanization intensity. The calculation methods for the three component indices: NDBI, SAVI, and MNDWI are presented in Equation 1 [26], Equation 2 [27], and Equation 3 [28], respectively:

$$NDBI = \frac{SWIR1 - NIR}{SWIR1 + NIR}$$

Equation 1

$$SAVI = \frac{(NIR - RED)(1 + L)}{NIR + RED + L}$$

Equation 2

$$MNDWI = \frac{GREEN - SWIR1}{GREEN + SWIR1}$$

Equation 3

In these equations, SWIR1, NIR, RED, and GREEN represent the shortwave infrared, near-infrared, red, and green spectral bands, respectively. For Landsat 8 imagery, these correspond to bands 6, 5, 4, and 3; while for Landsat 5 imagery, they correspond to bands 5, 4, 3, and 2, respectively. The IBI is designed to capture the three fundamental components of urban surfaces: vegetation, water, and impervious areas. Built-up regions typically exhibit higher IBI values compared to other land cover types. The IBI is computed using Equation 4 [29]:

$$IBI = \frac{NDBI - 0.5(SAVI + MNDWI)}{NDBI + 0.5(SAVI + MNDWI)}$$

Equation 4

Three IBI layers for the years 2000, 2010, and 2020 were generated to identify built-up areas based on their respective IBI value ranges. Two complementary approaches were applied to determine the optimal IBI threshold representing built-up areas. The first approach involved interpretation of satellite imagery, supported by historical imagery from Google Earth, to test multiple IBI value ranges and identify the most representative range for built-up areas. The second method is a field survey combined with quick interviews with local people and using GPS to collect information on areas that were built-up land in the past. In addition, land use status quo map in 2020 was also used to extract residential areas, then imported into GEE to support finding the appropriate IBI threshold of 2020.

### 2.3.2 Accuracy assessment

To evaluate the accuracy of the extracted built-up land layers, a total of 278 validation samples were employed. Specifically, the study identified long-established socio-economic structures such as Military Hospital No. 7, Hai Duong Museum, churches, pagodas, local government offices, schools, National Highway 37, markets, and other typical public facilities. In addition, brief interviews with local residents were conducted to verify the establishment periods of certain concentrated residential areas. The geographic coordinates of these reference sites were recorded using GPS devices for validation purposes. A total of 89 samples corresponded to the year 2000, 93 samples to 2010, and 96 samples to 2020. The 2020 samples were directly extracted from the land use status quo map and used to validate the classification results. The classification accuracy of the built-up land maps was assessed using the Overall Accuracy (OA) [30]. The OA measures the proportion of correctly classified samples relative to the total number of validation samples as presented in Equation 5:

$$OA = \frac{n}{N}$$

Equation 5

Where  $n$  is the number of correctly classified samples for class  $i$ ,  $k$  is the total number of classes, and  $N$  is the total number of validation samples. In addition, the Kappa Coefficient ( $\kappa$ ) was calculated to measure the level of agreement between the classification results and the reference data, taking into account the

possibility of agreement occurring by chance. The Kappa coefficient is defined in Equation 6:

$$\kappa = \frac{p_o - p_e}{1 - p_e}$$

Equation 6

Where  $p_o$  represents the observed agreement and  $p_e$  denotes the expected agreement by random chance [31].

### 2.3.3 Assessment of built-up area changes

In QGIS, built-up area distribution maps for the years 2000, 2010, and 2020 were overlaid to detect changes in built-up areas during the periods 2000-2010, 2010-2020, and 2000-2020. Prior to the overlay analysis, raster datasets were converted into vector format using the Polygonize (Raster to Vector) tool, and geometric errors in the resulting vector polygons were corrected with the Fix Geometries tool. This process aimed to accurately determine the built-up area of each commune and ward within Hai Duong City and to assess both spatial and temporal variations in urban expansion across the study periods. To quantify built-up area dynamics, the Symmetrical Difference operation was employed to overlay temporal layers and identify areas of change. In addition, several geoprocessing functions, including Difference (to detect variations), Dissolve (to aggregate features sharing common attributes), Clip (to extract features within the study boundary), and Merge Vector Layers (to integrate multiple datasets), were utilized to refine spatial analysis and ensure data consistency. The study workflow is illustrated in Figure 3.

## 3. Results and Discussion

### 3.1 Image Index Maps

The resulting index image layers are illustrated in Figure 4. The NDBI values for the entire study period range from -0.88 to 0.33. Specifically, Figure 4(a) shows the NDBI ranges for the years 2000, 2010, and 2020 are -0.88 to 0.26, -0.78 to 0.33, and -0.67 to 0.33, respectively. The SAVI index ranges from -0.17 to 0.65 across the entire period, with the annual distributions presented in Figure 4(b). The MNDWI values range from -0.64 to 0.91 for the whole period, with only minor variations between years, as shown in Figure 4(c). By combining the three indices: NDBI, SAVI, and MNDWI, using Equation 4, the IBI index layers were generated. The maximum IBI value was 0.21 in 2000, and 0.25 in both 2010 and 2020. Conversely, the minimum IBI values were -0.84 in 2000, -0.72 in 2010, and -0.61 in 2020. These results are presented in Figure 4(d).

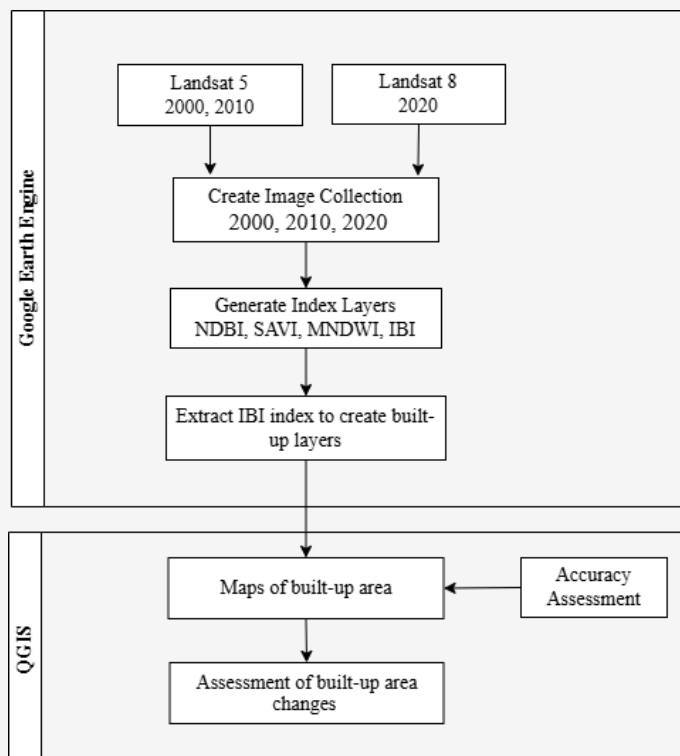


**Figure 3:** Built-up area change detection

### 3.2 Maps of built-up area

The threshold values determined for built-up land were  $IBI > 0.009$  in 2000,  $IBI > 0.035$  in 2010, and  $IBI > -0.09$  in 2020. A variation is observed among these threshold values, which can be attributed to differences in input data sources. Specifically, Landsat 5 imagery was employed for 2000 and 2010, whereas Landsat 8 imagery was used for 2020. In addition, each composite image was generated from multiple scenes, with a differing number of valid images per year, further contributing to this variation. Nevertheless, the difference remains relatively minor - the range between the maximum and minimum threshold values is only 0.044. Subsequently, built-up land maps for each year were generated, as presented in Figure 5. The classification accuracy was evaluated using confusion matrices that compared the built-up and non-built-up categories identified for 2000, 2010, and 2020 with corresponding reference samples. These matrices formed the basis for assessing classification performance, as presented in Table 1.

Based on the confusion matrix derived from reference samples, the classification accuracy was quantitatively evaluated for each temporal dataset. The results showed a high level of reliability across all study years. The overall accuracies (OA) for 2000, 2010, and 2020 were 88.76%, 89.25%, and 91.67%,

respectively, with corresponding Kappa coefficients of 0.76, 0.77, and 0.80. These results indicate that the classification maps are reliable, providing a sound basis for subsequent spatial and temporal analyses. As shown in Table 2, Hai Duong City experienced a remarkable expansion of built-up areas between 2000 and 2020, with particularly rapid growth after 2010, which is consistent with previous studies reporting significant increases in impervious surfaces across Vietnam's urban areas. In particular, built-up areas in Hai Duong Province expanded most rapidly between 2010 and 2022 [32], reinforcing the pattern identified in our study. Similar patterns of rapid urban expansion have also been documented in other Vietnamese cities such as Hai Phong and Can Tho during the same period [33], suggesting that the growth observed in Hai Duong reflects a broader trend of urbanization in Vietnam's urban and peri-urban regions. Collectively, these findings confirm the reliability of IBI in detecting built-up area dynamics and demonstrate its usefulness as a tool for monitoring urban growth in rapidly developing contexts. During the period from 2000 to 2010, the annual change in built-up area and the average urbanization rate were about 102.33 ha/year and 0.92%/year, respectively.

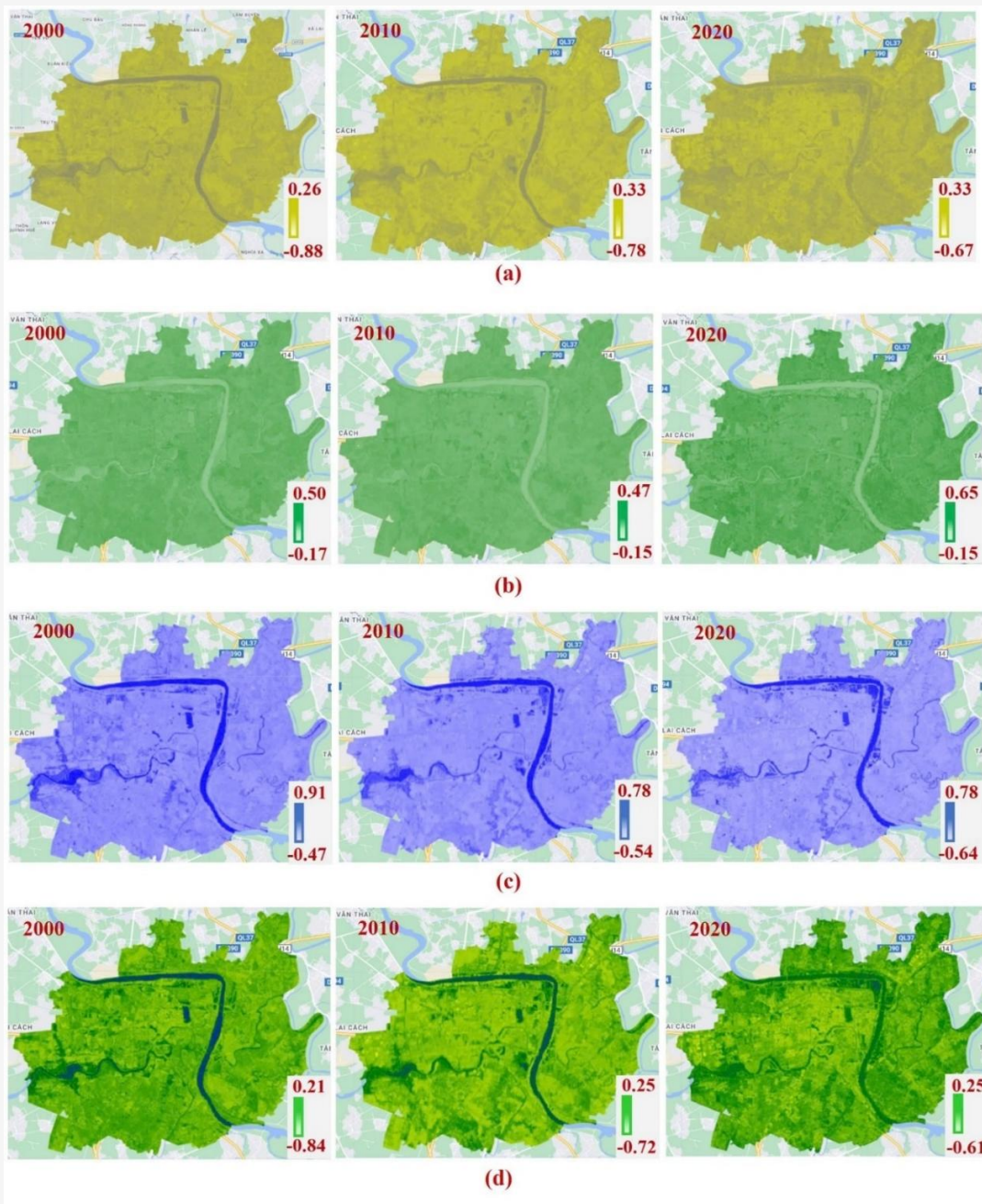


**Figure 4:** Spectral indices in 2000, 2010 and 2020: (a) NDBI, (b) SAVI, (c) MNDWI, and (d) IBI

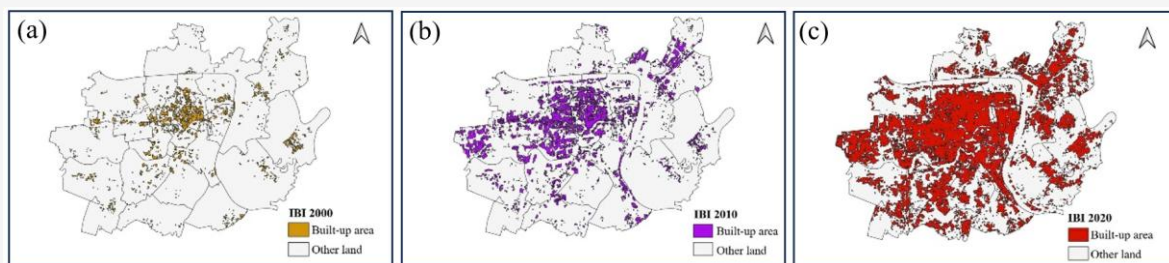


**Figure 5:** Maps of built-up area distribution in Hai Duong city: (a) in 2000, (b) in 2010 and (c) in 2020

**Table 1:** The confusion matrices

Year	Class	Built-up	Non-Built-up	Total
2000	Built-up	52	4	56
	Non-Built-up	6	27	33
2010	Built-up	55	3	58
	Non-Built-up	7	28	35
2020	Built-up	63	2	65
	Non-Built-up	6	25	31

**Table 2:** Area of built-up in years

Year	Built-up area (ha)	The ratio of built-up area to the total regional area (%)	The average annual change in built-up area (ha/year)	The average urbanization rate (%/year)
2000	474.04	4.24	-	-
2010	1497.32	13.41	102.33	0.92
2020	4432.83	39.69	293.55	2.63

From 2010 to 2020, these figures rose sharply to 293.55 ha/year and 2.63%/year, nearly three times higher than in the previous decade. Overall, the total proportion of built-up land increased by almost 9.4 times over 20 years, indicating a rapid and significant urbanization process. Accordingly, under the planning objectives toward 2030, Hai Duong is expected to become a modern industrial province with an urbanization rate exceeding 55% [34], which is entirely consistent with the trend of sustainable development and has a solid scientific basis. Furthermore, the master plan of Hai Duong City toward 2040 identifies the priority of developing green urban areas in key zones such as the central urban district, the areas along the Thai Binh and Sat rivers, and major transport corridors [35]. This aims to build Hai Duong City into a green, smart, and modern urban center. In this context, the city should ensure that land-use planning, technical infrastructure, and green urban development are implemented in a synchronized and integrated manner.

According to Figure 5, in 2000, the largest built-up area was in Binh Han ward, about 40.38 ha (accounting for 8.52% of the 2000 built-up area). In 2000, Gia Xuyen commune had the smallest built-up area of about 3.70 ha (accounting for 0.78% of the 2000 built-up area). In the next period, Tu Minh ward had the largest built-up area in 2010 and 2020 being 168.83 ha (accounting for 11.28% of the 2010 built-up area) and 455.55 ha (accounting for 10.28% of the 2020 built-up area), increasing by 437.73 ha in the whole period. In 2010 and 2020, Tran Hung Dao ward had the smallest built-up area with 20.52 ha (accounting for about 1.37% of the 2010 built-up area) and 31.49 ha (accounting for about 0.71% of the 2020 built-up area), respectively.

By administrative unit, in 2000, the built-up area ratio in Tran Hung Dao ward was the highest at 49.2%. In the central wards such as Nguyen Trai, Tran Phu, Quang Trung, Pham Ngu Lao, the built-up area ratio compared to the total natural area was about 30%, specifically 37.9%, 34.4%, 31.0% and 29.5%, respectively. Also, during this period, Binh Han, Le Thanh Nghi and Tan Binh wards began to urbanize with the built-up area ratio of 17.0%, 12.2% and 10.2%, respectively. At this stage, some communes have very small built-up area percentages, such as Gia Xuyen, An Thuong, Tan Hung, Nam Dong and Tien Tien communes with a ratio of less than 2%. In 2010, the built-up area was expanded, the wards in the central area all had a built-up area percentage of more than 45.0%, of which Nguyen Trai ward had the largest ratio of 67.4%. By 2020, the built-up area of the wards in the central area accounted for a very high ratio of over 80%. In particular, Ngoc Chau ward and Thanh Binh ward also had very high built-up areas, respectively 82.5% and 80.7%. In addition, there were 05 wards with a built-up area ratio of more than 55% compared to the total natural land area. The lowest built-up area ratio during this period was 17.8% located in Tien Tien ward (the ward with the largest natural land area in the city). Compared to 2000, the ward had a built-up area ratio that increased by 16.1%.

### 3.3 Assessment of Built-Up Area changes in the Period 2000 - 2020

Overlaying the layers of built-up area distribution maps of the years to determine the changes in built-up area in the periods 2000-2020, the results are shown in Table 3. In general, the built-up area in the period 2000-2020 has changed significantly.

**Table 3:** Built-up area changes in stages

No.	Wards/Communes	Total area of natural land	Built-up area changes 2000-2010	Built-up area changes 2010-2020	Built-up area changes 2000-2020
1	Ai Quoc	833.62	98.83	182.41	281.24
2	Binh Han	238.10	60.36	62.57	122.93
3	Cam Thuong	263.54	70.93	70.86	141.79
4	Hai Tan	411.54	28.07	236.21	264.28
5	Le Thanh Nghi	127.44	22.64	56.5	79.14
6	Nam Dong	889.49	69.59	205.78	275.37
7	Ngoc Chau	194.24	30.4	112.75	143.15
8	Nguyen Trai	55.90	16.48	15.91	32.39
9	Nhi Chau	316.75	20.24	80.11	100.35
10	Pham Ngu Lao	82.73	18.67	30.96	49.63
11	Quang Trung	104.31	16.85	34.76	51.61
12	Tan Binh	277.37	101.15	98.32	199.47
13	Tan Hung	502.22	19.04	173.85	192.89
14	Thach Khoi	545.72	43.75	167.89	211.64
15	Thanh Binh	262.82	82.57	109.86	192.43
16	Tran Hung Dao	35.67	2.99	10.97	13.96
17	Tran Phu	71.00	10.67	23.08	33.75
18	Tu Minh	737.96	151.01	286.72	437.73
19	Viet Hoa	651.11	46.46	134.42	180.88
20	An Thuong	664.15	19.97	102.04	122.01
21	Gia Xuyen	505.37	18.69	158.95	177.64
22	Lien Hong	934.53	20.23	165.63	185.86
23	Ngoc Son	486.99	34.81	83.74	118.55
24	Quyet Thang	898.00	7.34	169.04	176.38
25	Tien Tien	1,077.63	11.54	162.18	173.72
	Total	11,168.18	1,023.28	2,935.51	3,958.79

The total expanded built-up area in the period from 2000-2020 is 3,958.79 ha, accounting for 35.45% of the total land area. In these 20 years, Tu Minh ward has always had the largest change in built-up area with 437.73 ha (accounting for 11.06% of the total changed built-up area). Next are Nam Dong ward (accounting for 6.96% of the total) and Hai Tan ward (accounting for 6.68% of the total) with the fluctuating built-up area both over 264.00 ha. Tran Hung Dao ward has the smallest fluctuating built-up area with 13.96 ha, accounting for 0.35% of the total. Nguyen Trai ward and Tran Phu ward have the next smallest fluctuating built-up area with areas of 32.39 ha and 33.75 ha respectively. Next, three maps showing the change in construction area during the three phases are created.

In general, the built-up area in the period 2000-2020 has changed significantly. The total expanded built-up area in the period from 2000-2020 is 3,958.79 ha, accounting for 35.45% of the total land area. In these 20 years, Tu Minh ward has always had the largest change in built-up area with 437.73 ha (accounting for 11.06% of the total changed built-up area). Next are Nam Dong ward (accounting for 6.96% of the total) and Hai Tan ward (accounting for 6.68% of the total) with the fluctuating built-up area both over 264.00 ha. Tran Hung Dao ward has the smallest fluctuating built-up area with 13.96 ha, accounting for 0.35% of the total. Nguyen Trai ward and Tran Phu ward have the next smallest fluctuating built-up area with areas of 32.39 ha and 33.75 ha respectively. Next, three maps showing the change in construction area during the three phases are created.

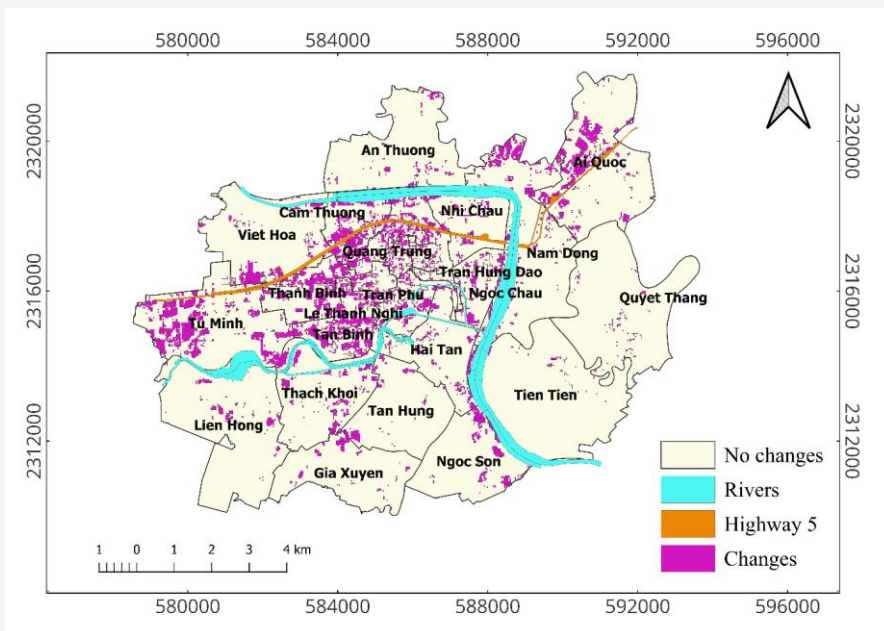


**Figure 6:** Built-up area changes map in the period 2000-2010

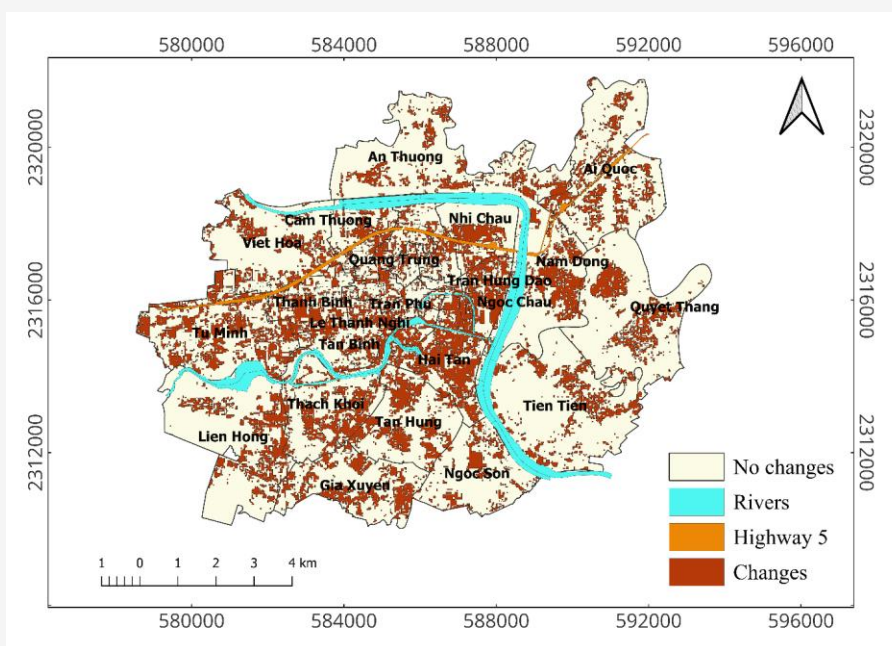


**Figure 7:** Built-up area changes map in the period 2010-2020

In the period 2000-2010, the total expanded built-up area was 1,023.28 ha. Of which, Tu Minh ward and Tan Binh ward have built-up area larger than 100 ha, specifically 151.01 ha and 101.15 ha respectively. In contrast, Quyet Thang commune and Tran Hung Dao ward have the smallest built-up area with an area of less than 10 ha. In particular, 18 out of 25 communes and wards have built-up area smaller than 50 ha. The changed built-up area is distributed as shown in Figure 6. In the next phase (2010 to 2020), Figure 7 illustrates that all communes and wards had

significantly increased built-up area. Specifically, the three communes and wards with the largest construction area all had an area of more than 200 hectares, Tu Minh ward had an area of nearly 300 hectares. The total built-up area in this phase was 2,935.51 hectares, nearly 3 times higher than the previous phase. In addition, the number of communes and wards with built-up area of less than 50 hectares was only 5 communes and wards. In addition, the number of communes and wards with areas larger than 100 hectares was 14.

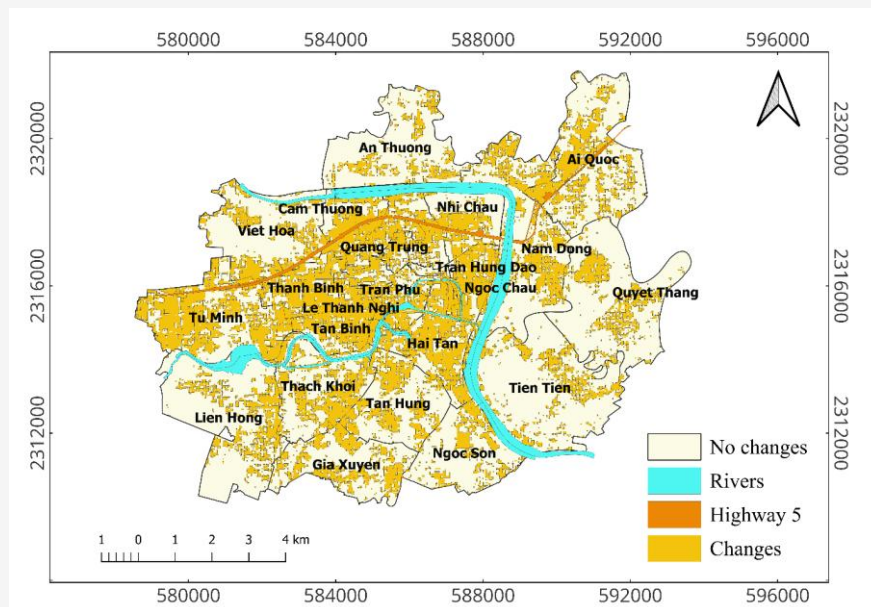


**Figure 8:** Built-up area changes map in the period 2000-2020

Figure 8 shows that in the 20 years from 2000-2020, the built-up area tends to increase sharply. The built-up area of the whole city accounts for 35.45% of the total land area. There are 10 communes and wards with built-up area accounting for more than 50% of the total natural land area. Of which, Tan Binh ward, Thanh Binh ward and Ngoc Chau ward have the built-up area ratio accounting for over 70% of the total natural land area with the respective ratios of 71.91%, 73.22% and 73.7%. During the period 2000-2010, the expansion of built-up land was mainly concentrated in the central area, moving westward, particularly around the intersection of National Highway 5 and the Sat River. In addition, areas along National Highway 5 toward Viet Hoa, Cam Thuong, and Binh Han wards also experienced a strong increase in built-up land. In the northeast of the city, along National Highway 5 in Ai Quoc ward, the built-up area expanded rapidly. Along the Thai Binh River to the south of the town, construction areas also grew significantly. The period 2010 to 2020 marked a rapid increase in built-up land, with urban expansion spreading more evenly from the city center to surrounding areas compared to the previous decade. The built-up land along the Thai Binh and Sat Rivers expanded substantially in Nam Dong, Ngoc Chau, and Hai Tan wards. Existing residential areas continued to grow and spread outward. Thus, between 2000 and 2020, Hai Duong City's urban network became more clearly defined, expanding from the existing urban core to neighboring areas. Built-up land in both inner and outer urban zones developed relatively evenly, forming a network

associated with economic corridors, major transportation routes, and large riverbanks. The expansion of built-up land along highways and rivers aligns with Hai Duong City's development orientation toward 2030 [34]. Overall, the increase in built-up land has contributed to shaping the urban network system, accelerating urbanization and modernization, and creating momentum for socio-economic development.

#### 4. Conclusion

This study assessed the spatial and temporal changes in built-up areas in Hai Duong City, Hai Duong Province, from 2000 to 2020. Hai Duong City has experienced a remarkable transformation characterized by the expansion of its urban space and the synchronized development of both technical and socio-economic infrastructure. In recent years, the proportion of built-up land has increased dramatically, reaching an average annual rate of 2.6% between 2010 and 2020. The total built-up area rose substantially from 474.04 hectares in 2000 to 4,432.83 hectares in 2020 - an almost 9.4-fold increase - clearly demonstrating a rapid yet sustainable urban expansion over the past two decades. During the 2000-2020 period, urban development was initially concentrated around the city center and progressively extended westward toward the intersection of National Highway No. 5 and the Sat River. At the same time, the expansion spread northeastward and southward along the Thai Binh River, creating an interconnected relationship between urban and riverine spaces.

The north-south development axis following National Highway No. 5 functions as a strategic corridor linking Hai Duong and Chi Linh - the province's two major urban centers as well as the district-level towns along the route, thereby enhancing inter-urban connectivity across the province. The east-west development direction along National Highway No. 5 has also witnessed the emergence of several industrial zones. In particular, the wards of Viet Hoa, Cam Thuong, Binh Han, Ngoc Chau, Thanh Binh, and Tan Binh have recorded significant increases in built-up land, confirming the city's pattern of coordinated and accelerated urban growth. The city's orientation toward 2040, Hai Duong, aims to prioritize the development of green urban areas in key zones such as the central urban district, the regions along the Thai Binh and Sat rivers, and major transport corridors. Nonetheless, the endeavor of constructing a green city will probably encounter several challenges, such as the impacts of quickly urban expansion, distinctions in urban planning and governance, and the necessity to align economic, cultural, and social advancement with environmental sustainability. Therefore, in the coming period, the city should continue to review and integrate existing planning frameworks, assess built-up land expansion, and restructure its spatial development strategy to ensure coherence and synchronization both spatially and temporally.

These findings clearly reflect the fast-paced and spatially uneven urbanization process in Hai Duong City. The results provide valuable insights for local authorities and urban planners in monitoring land use changes, identifying urban growth hotspots, and developing evidence-based strategies for sustainable urban development. Moreover, the approach demonstrated in this study can be applied to other rapidly urbanizing areas that require assessing urban expansion and supporting planning. In addition, the use of the Built-up index proved to be advantageous, as it highlights built-up areas with higher reliability compared to relying solely on individual indices such as NDVI or NDBI. By integrating spectral information from multiple bands, IBI enhances the discrimination between urban surfaces, bare land, and vegetation, thereby improving the detection and monitoring of urban changes over time.

The findings demonstrated that variations in satellite image quality had an impact on the precision of the study's results. Therefore, in the future research could utilize higher-resolution satellite data, such as Sentinel-2, or apply machine learning techniques to improve classification accuracy. Integrating remote sensing with socio-economic data would also provide deeper insights into the drivers and impacts of urban growth. Ultimately, Google

Earth Engine has proven to be an effective and adaptable platform, with expectations for its further use in studies of urban monitoring and planning as we advance.

## References

- [1] Viet, L. V., (2017). *Climate Change*, Ho Chi Minh City University of Industry.
- [2] Van, T. T., (2011). Application of Remote Sensing and GIS Monitoring Urbanization in Ho Chi Minh City through Impervious Surfaces. *Science & Technology Development*, Vol. 14(M1-2011), 66-77. <https://doi.org/10.32508/stdj.v14i1.1868>.
- [3] Almamalachy, Y. S., Al-Quraishi, A. M. F. and Moradkhani, H., (2019). Agricultural Drought Monitoring over Iraq Utilizing MODIS Products. *Environmental Remote Sensing and GIS in Iraq*: Springer, 253-278. [https://doi.org/10.1007/978-3-030-21344-2\\_11](https://doi.org/10.1007/978-3-030-21344-2_11).
- [4] Chen, J., (2007). Rapid Urbanization in China: A Real Challenge to Soil Protection and Food Security. *Catena*, Vol. 69(1), 1-15. <https://doi.org/10.1016/J.CATENA.2006.04.019>.
- [5] Witmer, R. E., (1978). US Geological Survey Land-Use and Land-Cover Classification System. *Journal of Forestry*, Vol. 76(10), 661-666. <https://doi.org/10.1093/jof/f%2F76.10.661>.
- [6] Ingels, F., Boyd, R., Bryant, E., Chapin, B., Jones, R. and Bouchillon, C., (1974). *A Study for the Application of Remote Sensing Data to Land Use Planning on the Mississippi Gulf Coast*. [Online]. Available: <https://ntrs.nasa.gov/api/citations/19740026620/downloads/19740026620.pdf>. [Accessed: Sep. 6, 2024].
- [7] Todd, W. J., (1977). Urban and Regional Land Use Change Detected by Using Landsat Data. *Journal of Research of the U.S. Geological Survey*, Vol. 5(5), 529-534. [Online]. Available: <https://pubs.usgs.gov/journal/1977/vol5issue5/report.pdf>. [Accessed: Sep. 8, 2024].
- [8] Horning, N., Fleishman, E., Ersts, P. J., Fogarty, F. A. and Wohlfeil Zillig, M., (2020). Mapping of Land Cover with Open-Source Software and Ultra-High-Resolution Imagery Acquired with Unmanned Aerial Vehicles. *Remote Sensing in Ecology and Conservation*, Vol. 6(4), 487-497. <https://doi.org/10.1002/rse2.144>.
- [9] Franklin, S. E., Ahmed, O. S., Wulder, M. A., White, J. C., Hermosilla, T. and Coops, N. C., (2015). Large Area Mapping of Annual Land Cover Dynamics Using Multitemporal Change Detection and Classification of Landsat Time

- Series Data. *Canadian Journal of Remote Sensing*, Vol. 41(4), 293-314. <https://doi.org/10.1080/07038992.2015.1089401>.
- [10] Tsuyuki, S., (2018). Completing Yearly Land Cover Maps for Accurately Describing Annual Changes of Tropical Landscapes. *Global Ecology and Conservation*, Vol. 13. <https://doi.org/10.1016/J.GECCO.2018.E00384>.
- [11] Thammaboribal, P., and Tripathi, N. (2024). Predicting Land Use and Land Cover Changes in Pathumthani, Thailand: A Comprehensive Analysis from 2013 to 2023 Using Landsat Satellite Imagery and CA-ANN Algorithm, with Projections for 2028 and 2038. *International Journal of Geoinformatics*, Vol. 20(5), 13–27. <https://doi.org/10.52939/ijg.v20i5.3225>.
- [12] Afrin, S., Gupta, A., Farjad, B., Ahmed, M. R., Achari, G. and Hassan, Q. K., (2019). Development of Land-Use/Land-Cover Maps Using Landsat-8 and MODIS Data, and their Integration for Hydro-Ecological Applications. *Sensors*, Vol. 19(22). <https://doi.org/10.3390/s19224891>.
- [13] Gorelick, N., Hancher, M., Dixon, M., Ilyushchenko, S., Thau, D. and Moore, R., (2017). Google Earth Engine: Planetary-Scale Geospatial Analysis for Everyone. *Remote Sensing of Environment*, Vol. 202, 18-27. <https://doi.org/10.1016/j.rse.2017.06.031>.
- [14] Kumar, L. and Mutanga, O., (2018). Google Earth Engine Applications Since Inception: Usage, Trends, and Potential. *Remote Sensing*, Vol. 10(10). <https://doi.org/10.3390/rs10101509>.
- [15] Thammaboribal, P. (2024). Investigating Land Surface Temperature Variation and Land Use Land Cover Changes in Pathumthani, Thailand (1997-2023) using Landsat Satellite Imagery: A Comprehensive Analysis of LST and Urban Hot Spots (UHS). *International Journal of Geoinformatics*, Vol. 20(2), 27–41. <https://doi.org/10.52939/ijg.v20i2.3063>.
- [16] Wang, S., Xu, M., Zhang, X. and Wang, Y., (2022). Fitting Nonlinear Equations with the Levenberg–Marquardt Method on Google Earth Engine. *Remote Sensing*, Vol. 14(9). <https://doi.org/10.3390/rs14092055>.
- [17] Wang, G., Peng, W., Zhang, L., Xiang, J., Shi, J. and Wang, L., (2023). Quantifying Urban Expansion and its Driving Forces in Chengdu, Western China. *The Egyptian Journal of Remote Sensing and Space Sciences*, Vol. 26(4), 1057-1070. <https://doi.org/10.1016/j.ejrs.2023.11.010>.
- [18] Estoque, R. C. and Murayama, Y., (2015). Classification and Change Detection of Built-Up Lands from Landsat-7 ETM+ and Landsat-8 OLI/TIRS Imageries: A Comparative Assessment of Various Spectral Indices. *Ecological Indicators*, Vol. 56, 205-217. <https://doi.org/10.1016/J.ECOLIND.2015.03.037>.
- [19] Sinha, P., Verma, N. K. and Ayele, E., (2016). Urban Built-Up Area Extraction and Change Detection of Adama Municipal Area Using Time-Series Landsat Images. *International Journal of Advanced Remote Sensing and GIS*, Vol. 5(8), 1886-1895. <https://doi.org/10.23953/CLOUD.IJARSG.67>.
- [20] Fang, H., Wei, Y. and Dai, Q., (2019). A Novel Remote Sensing Index for Extracting Impervious Surface Distribution from Landsat 8 OLI Imagery. *Applied Sciences*, Vol. 9(13). <https://doi.org/10.3390/APP9132631>.
- [21] Prasomsup, W., Piyatadsananon, P., Aunphoklang, W. and Boonrang, A., (2020). Extraction Technic for Built-Up Area Classification in Landsat 8 Imagery. *International Journal of Environmental Science and Development*, Vol. 11(1), 15-20. <https://doi.org/10.18178/ijesd.2020.11.1.1219>.
- [22] Hanh, N. T. T., (2019). Applying Urban Indices to Extract Bare Land and Buid-Up Areas in Hanoi from Landsat 8. *Journal of Mining and Earth Sciences*, Vol. 60(4), 82-90. <https://tapchi.humg.edu.vn/en/archives?article=1028>.
- [23] Chinh, D. T. M., Thao, D. T. P. and Hai, N. M., (2021). Using Index-Base Built-Up Index (IBI) from Multi-Temporal Remote Sensing Data to Monitor the Urbanization of Nha Trang City in Vietnam. *Journal of Science on Natural Resources and Environment*, Vol. 38, 74-82. <https://tapchikhtnmt.hunre.edu.vn/index.php/tapchikhtnmt/article/view/364>.
- [24] Loi, N. T. and Tuan, V. Q., (2021). Urban Land Classification Using Index Images Based on Sentinel-2 Images - A Case Study in Long Xuyen City, Ca Mau City and Ninh Kieu District. *CTU Journal of Science*, Vol. 57(2), 190-201. <https://doi.org/10.22144/ctu.jsci.2021.062>.
- [25] *Hai Duong City Statistical Yearbook 2023*. (2024). Hai Duong Provincial Statistics Office. *Hai Duong City Statistical Yearbook 2023*. <https://thongkeh.gov.vn/phat-hanh-nien-giam-thong-ke-2023-tinh-hai-duong/>.

- [26] Zha, Y., Gao, J. and Ni, S., (2003). Use of Normalized Difference Built-Up Index in Automatically Mapping Urban Areas from TM Imagery. *International Journal of Remote Sensing*, Vol. 24(3), 583-594. <https://doi.org/10.1080/01431160304987>.
- [27] Huete, A. R., (1988). A Soil-Adjusted Vegetation Index (SAVI). *Remote Sensing of Environment*, Vol. 25(3), 295-309. <https://doi.org/10.1016/0034-4257%2888%2990106-X>.
- [28] Xu, H., (2006). Modification of Normalised Difference Water Index (NDWI) to Enhance Open Water Features in Remotely Sensed Imagery. *International Journal of Remote Sensing*, Vol. 27(14), 3025-3033. <https://doi.org/10.1080/01431160600589179>.
- [29] Bektaş Balçık, F., (2014). Determining the Impact of Urban Components on Land Surface Temperature of Istanbul by Using Remote Sensing Indices. *Environmental Monitoring and Assessment*, Vol. 186(2), 859-872. <https://doi.org/10.1007/s10661-013-3427-5>.
- [30] Ursu, C. D., Benedek, J. and Temerdeş-Ivan, K., (2025). Accuracy Assessment of Four Land Cover Datasets at Urban, Rural and Metropolitan Area Level. *Remote Sensing*, Vol. 17(5). <https://doi.org/10.3390/rs17050756>.
- [31] Khan, S., Bhardwaj, A. and Sakthivel, M., (2024). Accuracy Assessment of Land Use Land Cover Classification Using Machine Learning Classifiers in Google Earth Engine; A Case Study of Jammu District. *The International Archives of the Photogrammetry, Remote Sensing and Spatial Information Sciences*, Vol. 48, 263-268. <https://doi.org/10.5194/isprs-archives-XLVIII-4-2024-263-2024>.
- [32] Thien, B. B., Ovsepyan, A. E. and Phuong, V. T., (2024). Monitoring Land Surface Temperature Relationship to Land Use and Land Cover in Hai Duong Province, Vietnam. *Environment and Natural Resources Journal*, Vol. 22(2), 145-157. <https://doi.org/10.32526/enrj%2F22%2F20230194>.
- [33] Tuan, N. T., (2023). A Comparative Study of Urban Land Use Efficiency of the Cities of Hai Phong and Can Tho, Vietnam. *Environmental & Socio-economic Studies*, Vol. 11, 43 - 53. <https://doi.org/10.2478/enviro-2023-0016>.
- [34] Thao, A., (2024). By 2030, Hai Duong Strives to Achieve an Urbanization Rate of over 55%. *Journal of Construction*. <https://tapchixaydung.vn/den-nam-2030-hai-duong-phan-dau-dat-tile-do-thi-hoa-tren-55-20201224000021495.html>.
- [35] Viet, N., (2025). Hai Duong: Towards a Green, Smart, Modern and Sustainable City. *Institute of Strategy and Policy on Agriculture and Environment - Ministry of Agriculture and Environment - Mae*. <https://tapchimoitruong.vn/chuyen-muc-3/hai-duong-huong-toi-do-thi-xanh-thong-minh-hien-dai-va-ben-vung-31571>.